Supporting Information

Synergizing PIERS and Photocatalysis Effects in a Photo-responsive Ag/TiO_2 Nanostructure for an Ultrasensitive and Renewable PI-PC SERS Technique

Quan-Doan Mai[a,*], Dang Thi Hanh Trang[a], Ta Ngoc Bach[b], Vo Thi Le Na[c], Anh-Tuan Pham[c], Anh-Tuan Le[a,c,**]

[a]*Phenikaa University Nano Institute (PHENA), Phenikaa University, Hanoi 12116, Vietnam*
[b]*Institute of Materials Science (IMS), Vietnam Academy of Science and Technology, 18 Hoang Quoc Viet, Hanoi 10000, Vietnam*
[c]*Faculty of Materials Science and Engineering (MSE), Phenikaa University, Hanoi 12116, Vietnam*

Corresponding authors:

*doan.maiquan@phenikaa-uni.edu.vn (Q.D. Mai)

**tuan.leanh@phenikaa-uni.edu.vn (A.T. Le)

Calculation of limit of detection (LOD)

The LOD value was calculated based on the linear equation established for each technique (SERS, PI-PC SERS) and the Raman signal of the corresponding analyte in its powder form. The LOD is calculated using the following equation(1):

$$LOD = 10^{\left[\left(Y_{average} + 3SD\right)/Y_{average} - A\right]/B} \quad (1)$$

Here, $Y_{average}$ represents the average Raman intensity derived from 10 repeated measurements of the analyte (MB or thiram) in its powder form. SD is the standard deviation of the Raman signal, calculated from 10 measurements using the formula provided below. A and B are the intercept and slope, respectively, of the linear equation obtained by plotting the logarithmic SERS intensity (y) against the logarithmic concentration (x), expressed as (y = A + B*x).

SD is calculated via the well-known formula:

$$SD = \sqrt{\frac{1}{n-1} \times \sum_{i}^{n} (Y_i - Y_{average})^2} \quad (2)$$

where n=10 is the number of measurements, Y_i is the Raman intensity recorded during the i^{th} measurement, and $Y_{average}$ is the mean Raman intensity obtained from the 10 repeated measurements of the analyte (MB or thiram) in powder form.

Calculation of relative standard deviation (RSD)

The RSD value of repeatability and reproducibility is calculated via the well-known formula:

$$\text{RSD} = \frac{SD \times 100}{x_{average}} \quad (3)$$

where SD is the standard deviation that calculates using equation 2 and $x_{average}$ is the average value of SERS signal obtained from each measurement.

Table S1. Assignments of vibrational bands in SERS spectrum of MB.

SERS peak (cm^{-1})	Peak assignment
460	δ(C-N-C) + δ(C-S-C) (2, 3)
508	δ(C-N-C) + δ(C-S-C) (2, 3)
1120	δ(C-H) (2, 3)
1410	ν_{as}(C-N) (2, 3)
1615	ν_{s}(C-C) (2, 3)

δ = bending; ν_s = symmetric stretching; ν_{as} = antisymmetric stretching.

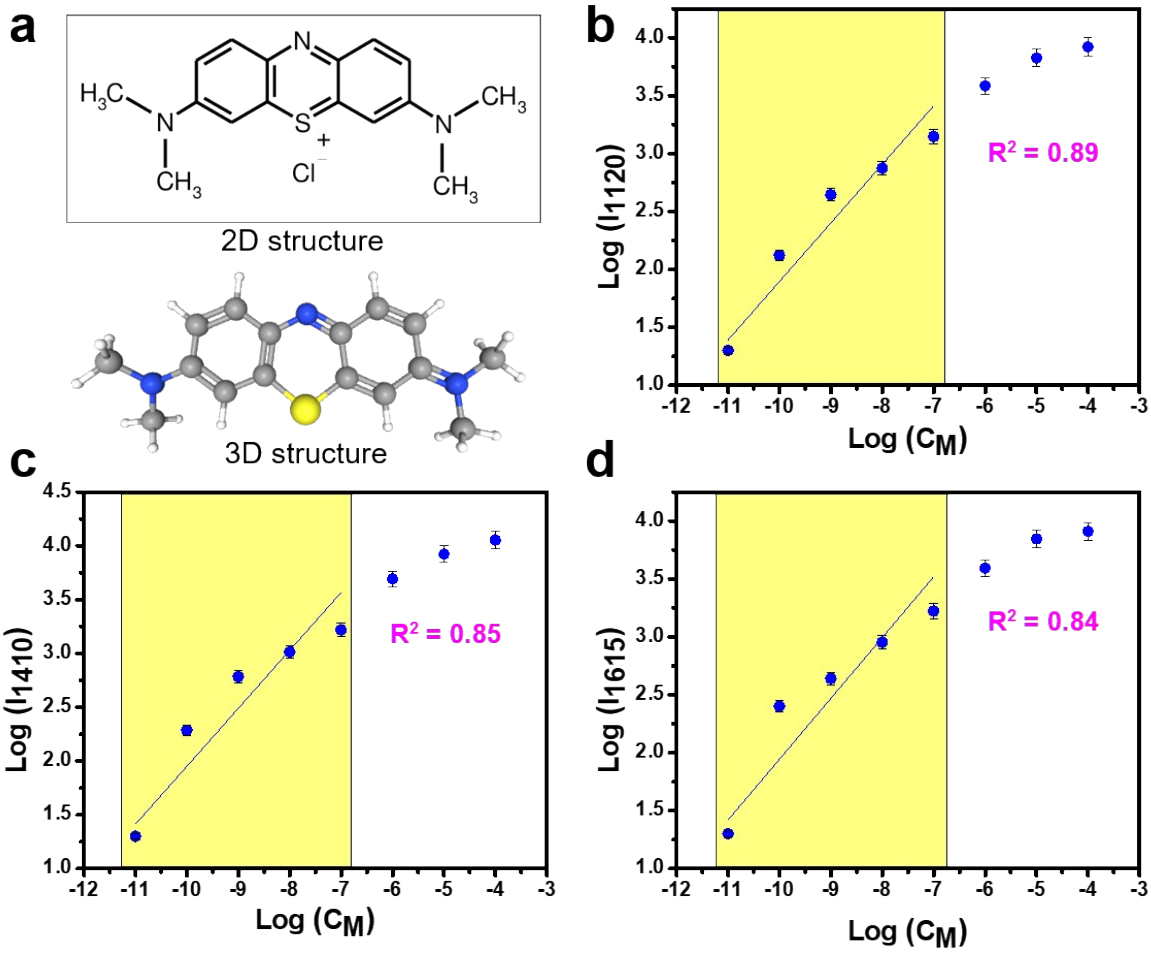

Figure S1. Tow-dimensional (2D) and three-dimensional (3D) molecular structures of methylene blue (MB) (a), and the linear relationship between concentration and SERS intensity plotted on a logarithmic scale at the peaks 1120 cm^{-1} (b), 1410 cm^{-1} (c), and 1615 cm^{-1} (d) of MB.

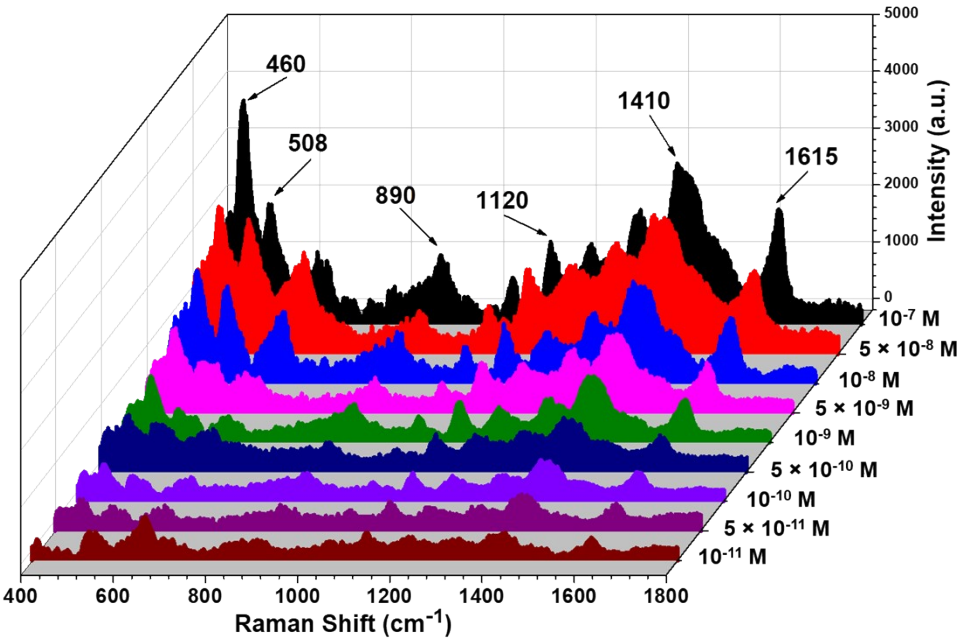

Figure S2. SERS spectra of MB in the concentration range of 10^{-7} M to 10^{-11} M with a two-fold step decrease under normal SERS conditions.

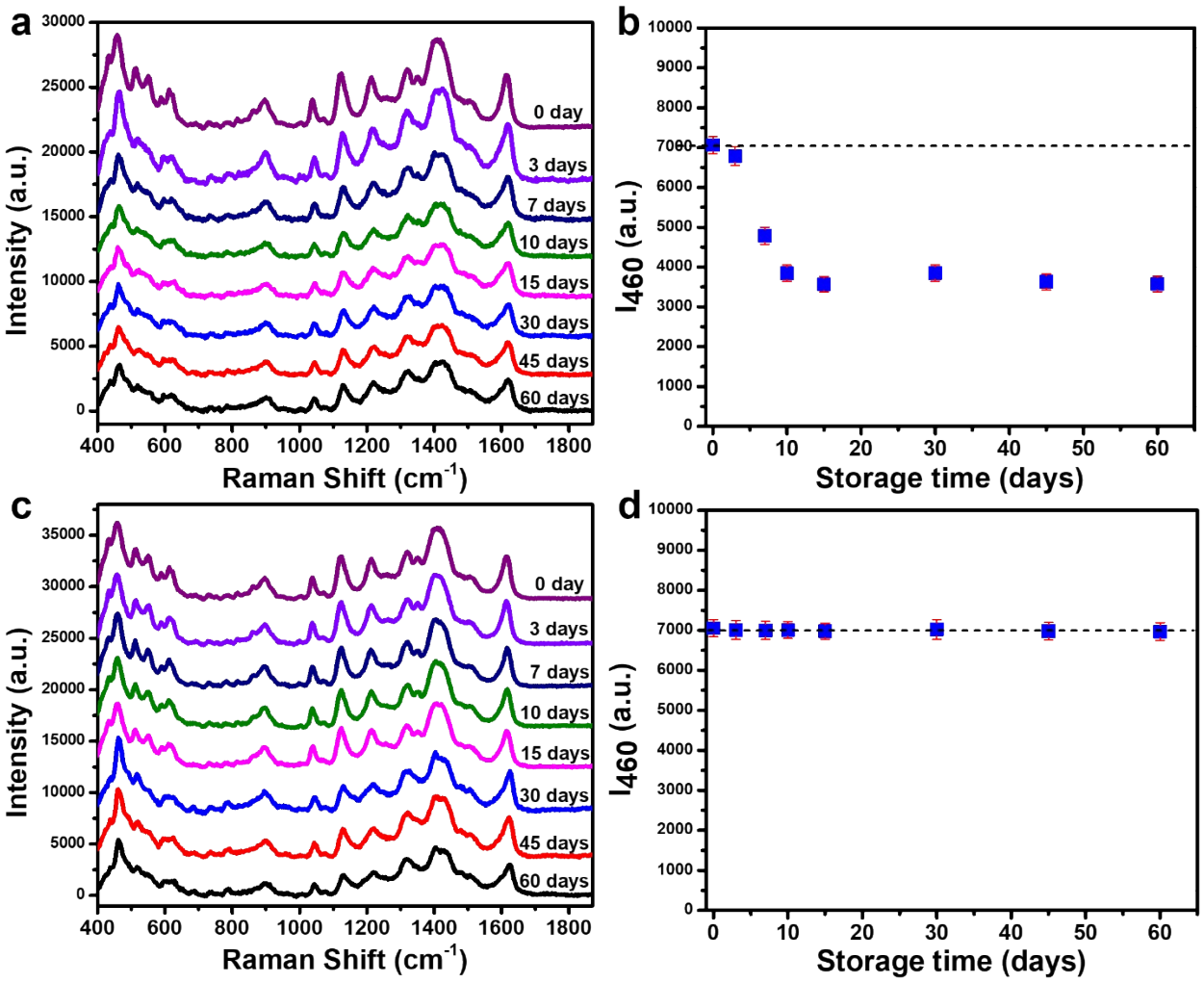

Figure S3. Stability of the SERS signal of MB at a concentration of 10^{-6} M on the Ag/TiO_2 substrate under two storage conditions: (a) in a laboratory environment (exposed to moisture and light), and (b) in a sealed container (protected from moisture and light).

The long-term stability of the Ag/TiO_2 substrate is essential for evaluating its practical applications, particularly when utilizing the PIERS and photocatalysis effects in the PI-PC SERS technique. To assess this, the stability of the Ag/TiO_2 substrate was evaluated by monitoring the SERS signal of MB at a concentration of 10^{-6} M over 60 days under two storage conditions: (i) a laboratory environment (exposed to moisture and light) and (ii) a sealed container (protected from moisture and light). SERS signals were recorded at specific intervals of 3, 7, 10, 15, 30, 45, and

60 days after fabrication and compared to the signals collected immediately after fabrication. The results are presented in Figure S3. Under laboratory storage conditions, where the substrate was directly exposed to air and light, the Ag/TiO_2 substrate exhibited relatively good stability over 60 days (Figure S3a). The characteristic peaks of MB appeared clearly and showed no positional shifts across all time points. However, the intensity of these peaks gradually decreased from day 3 to day 15. Figure S3b illustrates the changes in intensity at the 460 cm^{-1} peak. While the SERS signals remained largely unchanged after 3 days of storage, a notable decline was observed at 7, 10, and 15 days. This reduction is likely due to the direct exposure of Ag/TiO_2 to moisture and light, which may have caused oxidation of the Ag component(4). After day 15, the SERS signals stabilized and were maintained consistently until day 60. These results suggest that, although the Ag/TiO_2 substrate retained its ability to detect MB over the 60-day storage period, the reduced signal intensity under direct exposure to oxidative factors such as moisture and light could compromise its sensing performance. To mitigate these effects, additional experiments were conducted by storing the Ag/TiO_2 substrate in a sealed container, protecting it from moisture and light. Figure S3c presents the SERS spectra recorded over various time points, while Figure S3d highlights the stability of the 460 cm^{-1} peak intensity. The results show that the substrate exhibited excellent stability over the 60-day period. The characteristic peaks remained well-defined, and their intensities showed no significant changes throughout the storage duration. These results show that storing the Ag/TiO_2 substrate in a sealed container is suitable for maintaining its stability while ensuring practicality during experiments.

Table S2. Comparison of SERS and PI-PC SERS enhancements for MB at 460 cm^{-1}.

MB Concentration	Peak Intensity (a.u.) (SERS)	Peak Intensity (a.u.) (PI-PC SERS)	Enhancement comparison (PI-PC SERS/SERS)
10^{-4} M	12266	16608	1.35
10^{-5} M	10812	14923	1.38
10^{-6} M	6664	13310	2.00
10^{-7} M	3301	11828	3.58
10^{-8} M	1275	8150	6.39
10^{-9} M	486	3889	8.00
10^{-10} M	202	1778	8.80

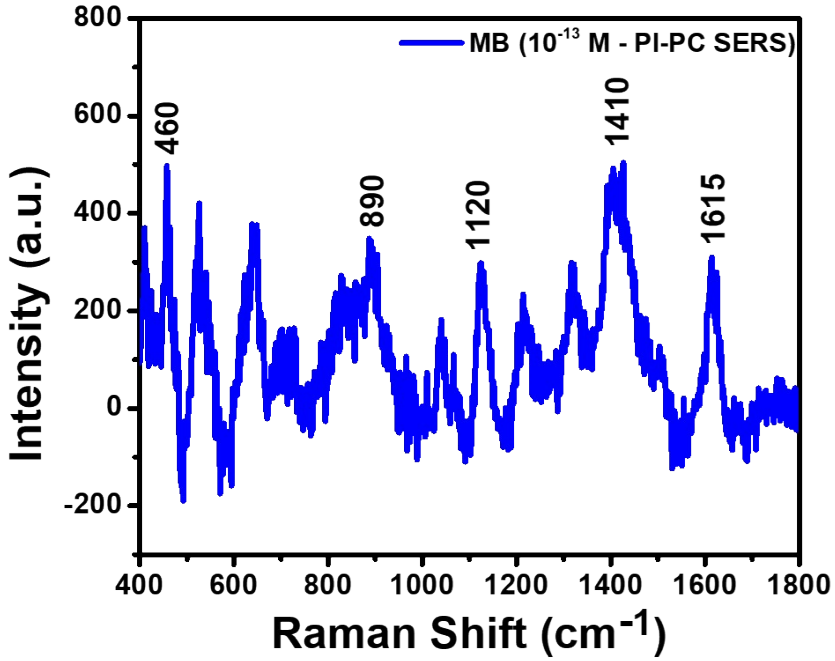

Figure S4. SERS spectrum of MB at a concentration of 10^{-13} M collected using the PI-PC SERS technique.

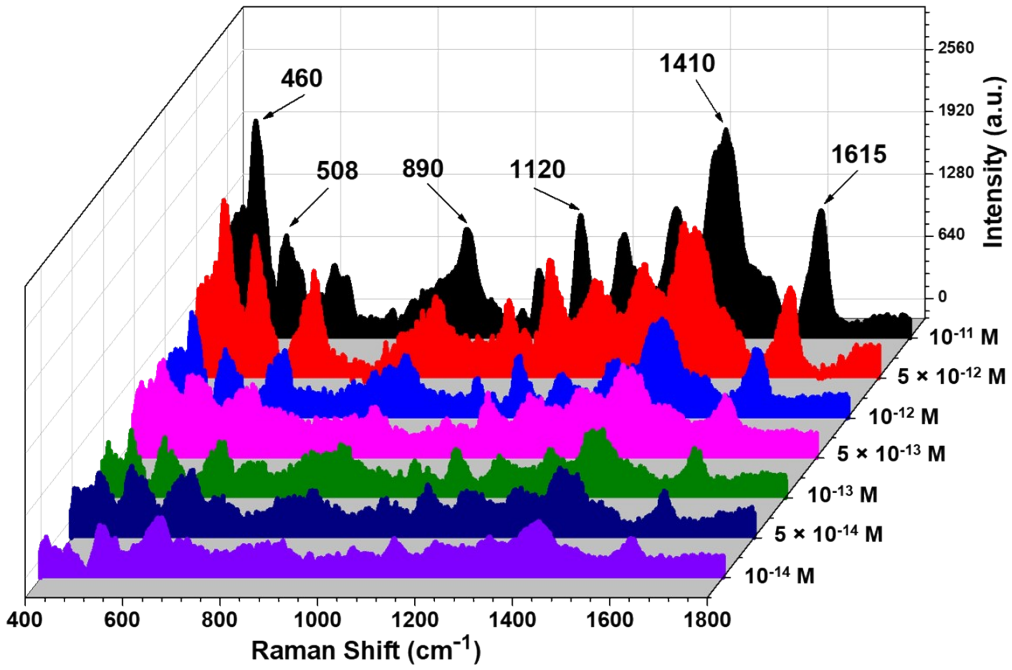

Figure S5. SERS spectra of MB in the concentration range of 10^{-11} M to 10^{-14} M with a two-fold step decrease under PI-PC SERS technique.

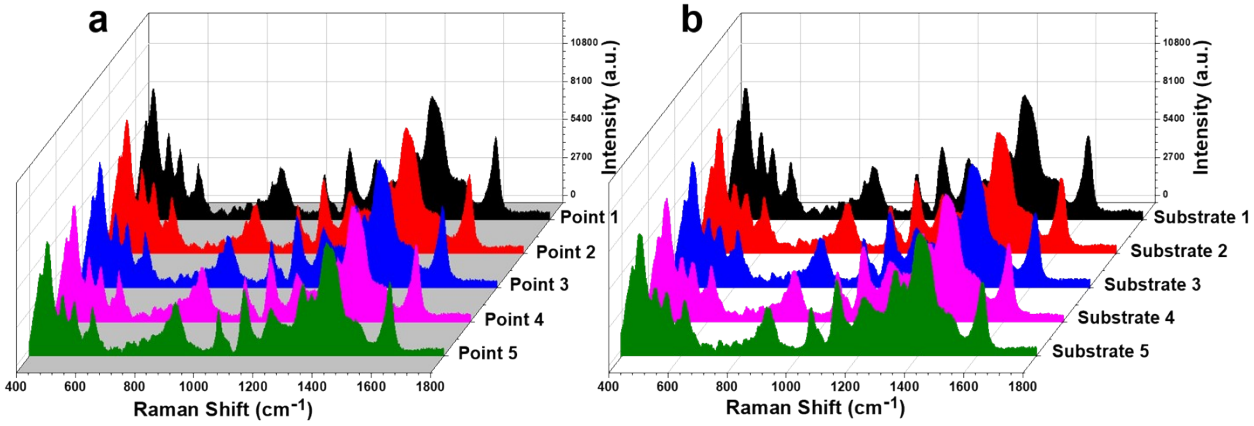

Figure S6. Evaluation of the reliability of the PI-PC SERS experiment for MB detection at concentrations of 10^{-8} M through repeatability (a) and reproducibility (b).

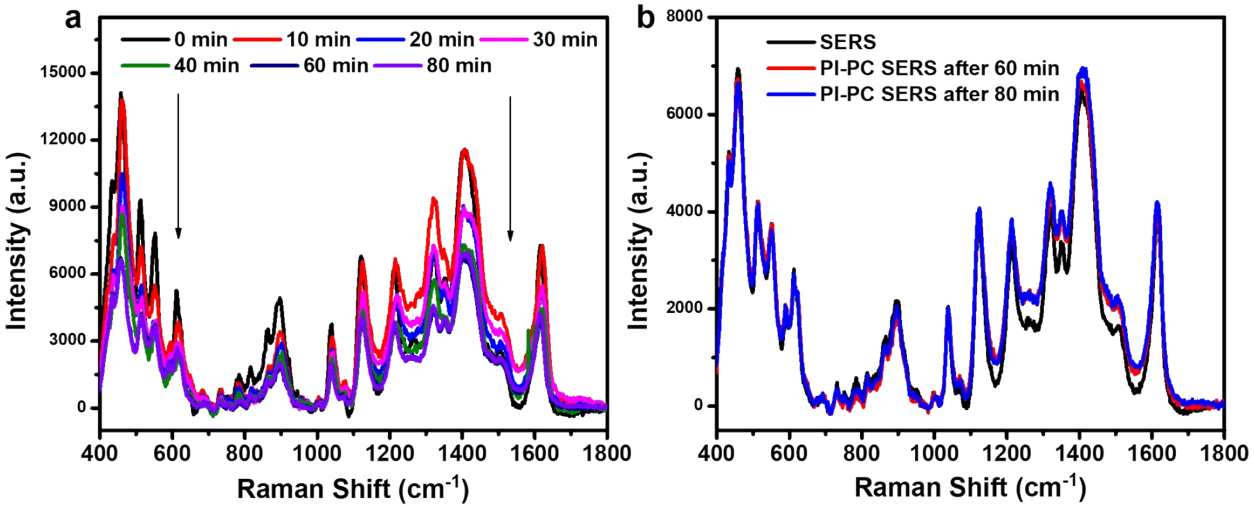

Figure S7. Evaluation of the stability of the PIERS effect on the Ag/TiO_2 substrate after the pre-irradiation process, using SERS spectra of MB at a concentration of 10^{-6} M collected at various time intervals (a) and compares the SERS signal intensity of MB at a concentration of 10^{-6} M between normal SERS and PI-PC SERS after 60 and 80 minutes of exposure to air (b).

The spectrum at 0 minutes was recorded immediately after the pre-irradiation process and the addition of MB at a concentration of 10^{-6} M. Subsequent SERS spectra were collected after 10 minutes of exposure to air. The data show that the SERS intensity after 10 minutes of air exposure for the Ag/TiO_2 substrate decreased only slightly compared to the spectra obtained immediately after pre-irradiation. However, the spectra at the 20-minute mark exhibited a significant reduction in intensity at all characteristic peaks. This gradual decrease continued at subsequent time points of 30, 40, and 60 minutes (Figure S6a). By 80 minutes after pre-irradiation, the SERS intensity had stabilized, indicating that the signal reduction had plateaued. Notably, the SERS spectra at the 60-minute and 80-minute marks were similar in intensity to those obtained using normal SERS technique for MB at a concentration of 10^{-6} M (Figure S6b). This indicates that after a sufficient exposure time to air (60 minutes), the PIERS effect on the Ag/TiO_2 substrate was entirely diminished, reverting to the normal SERS effect. This phenomenon likely results from the recovery of oxygen vacancies on the TiO_2 surface due to the filling of oxygen from the air. Therefore, to achieve optimal performance when applying the PI-PC SERS technique, SERS spectra in this study were collected immediately after the pre-irradiation and the analyte addition process.

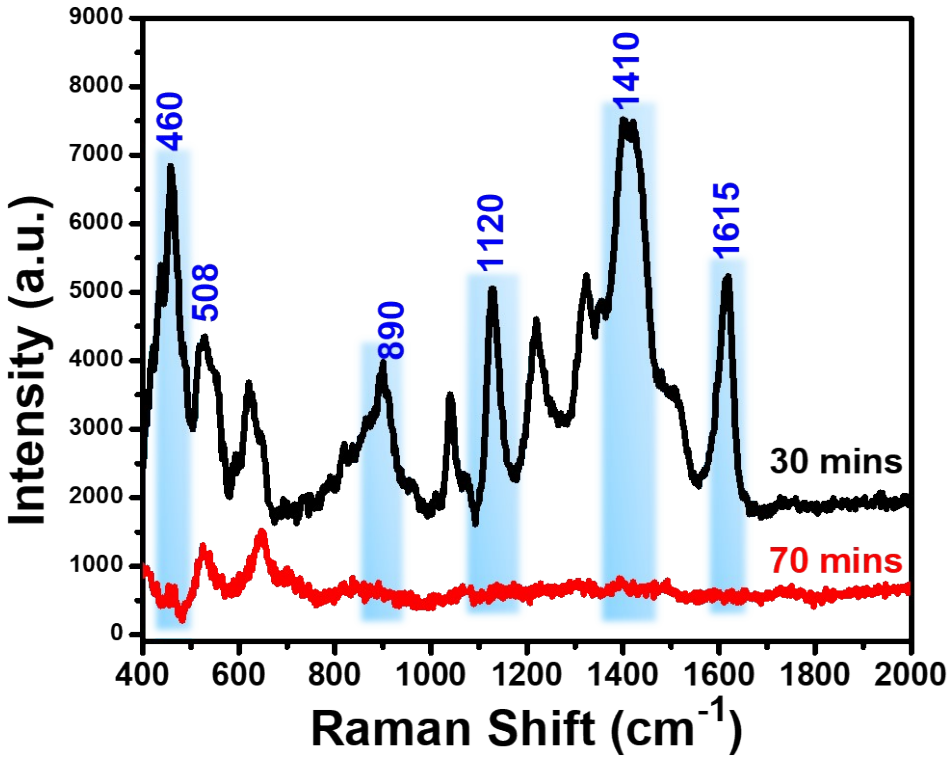

Figure S8. SERS spectra of Ag/TiO_2 substrate collected during photocatalytic degradation of MB, comparing the efficiency between 30 minutes and 70 minutes of photocatalytic process.

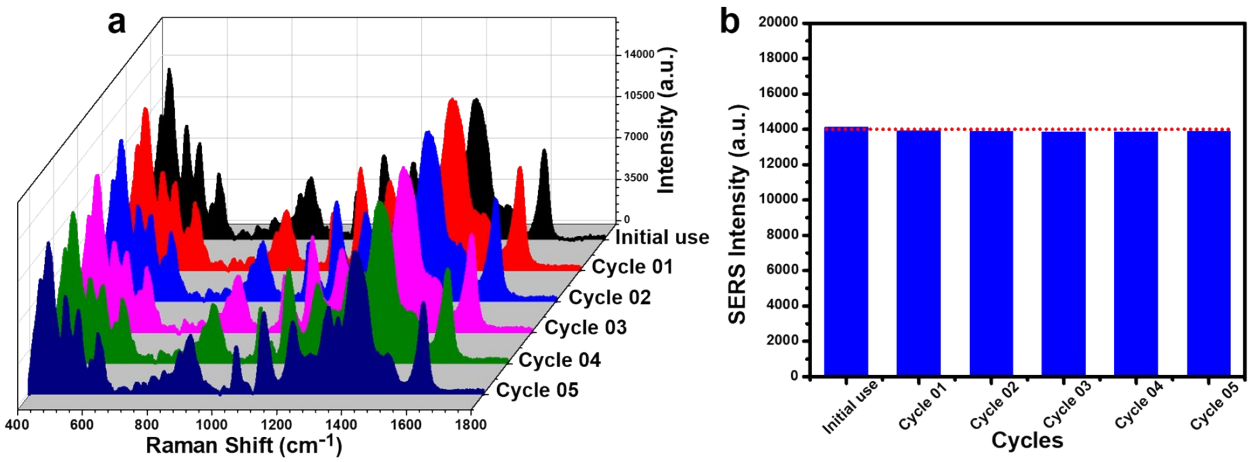

Figure S9. Evaluation of the cyclability of the PI-PC SERS technique over five different cycles. It compares the SERS spectra of MB at a concentration of 10^{-6} M obtained on the Ag/TiO_2 substrate during the initial use with those from the subsequent five cycles (a), and compares the SERS intensity at the 460 cm^{-1} peak for MB at a concentration of 10^{-6} M between the initial use and the five subsequent cycles (b).

Table S3. Assignments of vibrational bands in SERS spectrum of thiram.

SERS peak (cm^{-1})	Peak assignment
450	ν_s(CSS) (5), δ(C–N–C) (6)
570	ν(S–S) + ν_s(CSS) (5-7)
860	ν_{as}(CH_3-N) (5, 7)
1150	ρ(CH_3) + ν(N–CH_3) (6-8)
1386	δ(CH_3), ν(C-N) (5, 7)

δ = bending; ρ = rocking; ν_s = symmetric stretching; ν_{as} = antisymmetric stretching.

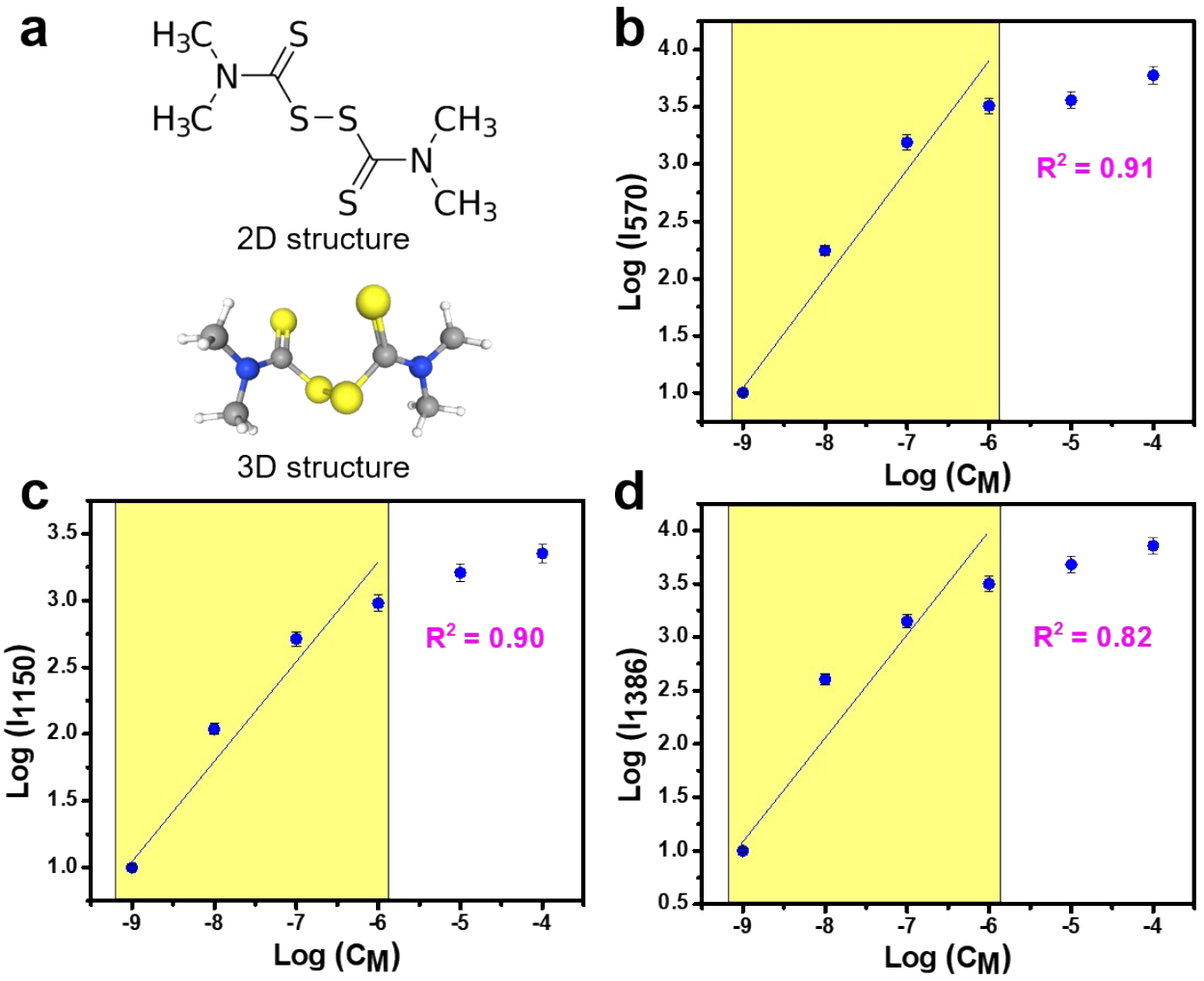

Figure S10. Tow-dimensional (2D) and three-dimensional (3D) molecular structures of thiram (a), and the linear relationship between concentration and SERS intensity plotted on a logarithmic scale at the peaks 570 cm^{-1} (b), 1150 cm^{-1} (c), and 1386 cm^{-1} (d) of thiram.

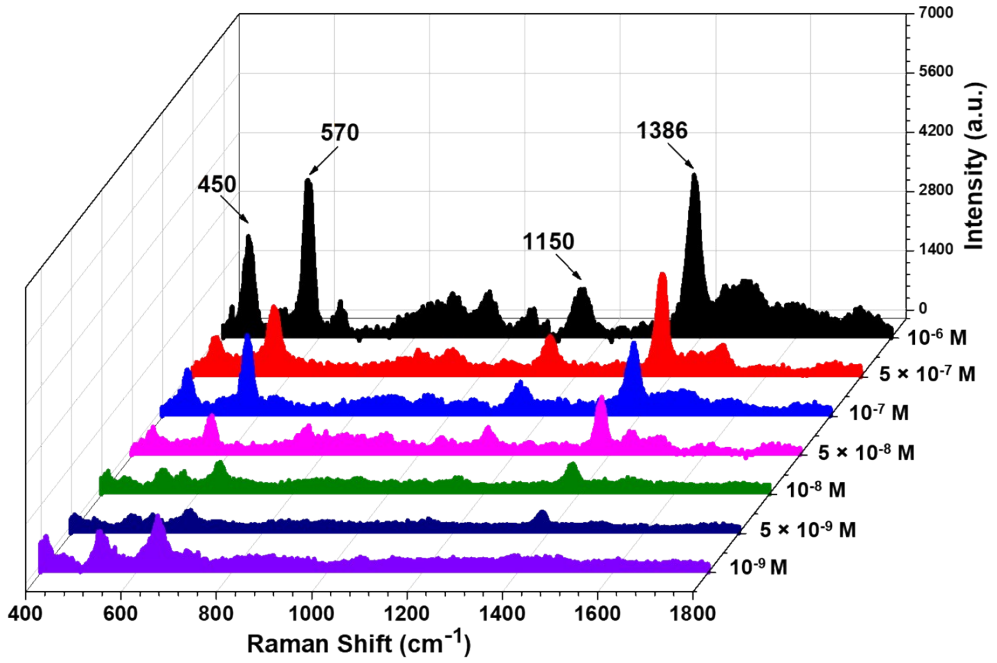

Figure S11. SERS spectra of thiram in the concentration range of 10^{-6} M to 10^{-9} M with a two-fold step decrease under normal SERS conditions.

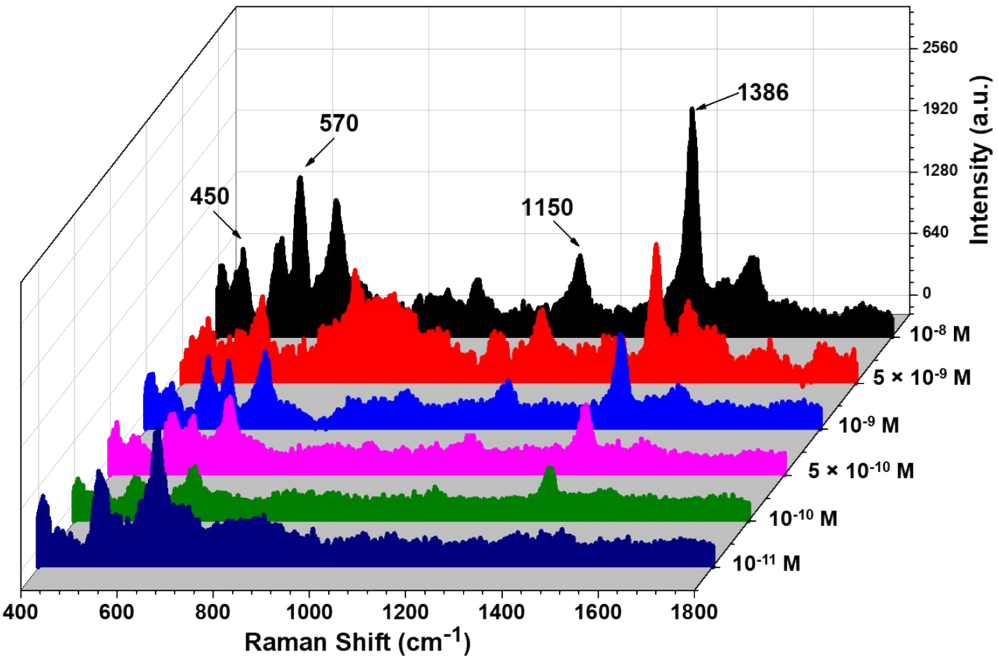

Figure S12. SERS spectra of thiram in the concentration range of 10^{-8} M to 10^{-11} M with a two-fold step decrease under PI-PC SERS technique.

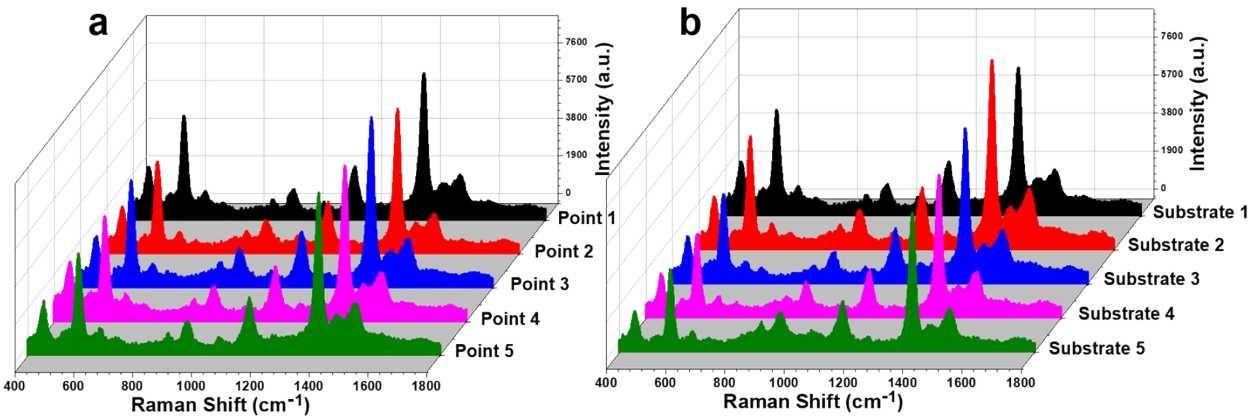

Figure S13. Evaluation of the reliability of the PI-PC SERS experiment for thiram detection through repeatability (a) and reproducibility (b).

References

1. Chen R, Shi H, Meng X, Su Y, Wang H, He Y. Dual-amplification strategy-based SERS chip for sensitive and reproducible detection of DNA methyltransferase activity in human serum. Analytical chemistry. 2019;91(5):3597-603.

2. Ruan C, Eres G, Wang W, Zhang Z, Gu B. Controlled fabrication of nanopillar arrays as active substrates for surface-enhanced Raman spectroscopy. Langmuir. 2007;23(10):5757-60.

3. Virdee H, Hester R. Surface-Enhanced Raman Spectroscopy of Thionine-modified Gold Electrodes. Laser chemistry. 1988;9(4-6):401-16.

4. Matikainen A, Nuutinen T, Itkonen T, Heinilehto S, Puustinen J, Hiltunen J, et al. Atmospheric oxidation and carbon contamination of silver and its effect on surface-enhanced Raman spectroscopy (SERS). Scientific reports. 2016;6(1):37192.

5. Kang J-S, Hwang S-Y, Lee C-J, Lee M-S. SERS of dithiocarbamate pesticides adsorbed on silver surface; Thiram. Bulletin of the Korean Chemical Society. 2002;23(11):1604-10.

6. Oliveira MJ, Martin CS, Rubira RJ, Batagin-Neto A, Constantino CJ, Aroca RF. Surface-enhanced Raman scattering of thiram: quantitative and theoretical analyses. Journal of Raman Spectroscopy. 2021;52(12):2557-71.

7. Sanchez-Cortes S, Domingo C, García-Ramos J, Aznárez J. Surface-enhanced vibrational study (SEIR and SERS) of dithiocarbamate pesticides on gold films. Langmuir. 2001;17(4):1157-62.

8. Ding Y, Zhang X, Yin H, Meng Q, Zhao Y, Liu L, et al. Quantitative and sensitive detection of chloramphenicol by surface-enhanced Raman scattering. Sensors. 2017;17(12):2962.